



When less is more: Enhancement of green hydrogen production and efficiency by using electrodes with ultra-low platinum loadings

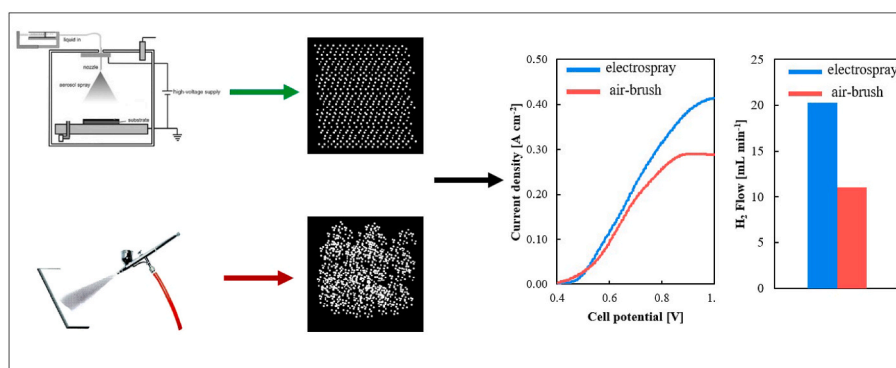
Sergio Diaz-Abad, Iñaki Requena, Manuel A. Rodrigo, Justo Lobato*

Chemical Engineering Department, Enrique Costa Building, University of Castilla-La Mancha, Av. Camilo Jose Cela n 12, Ciudad Real, 13071, Spain

HIGHLIGHTS

- Electro spray enhances SDE performance due to improved catalyst dispersion.
- Reducing platinum loading 7 times in the cathode boosted hydrogen production.
- The H₂ purity is increased one order of magnitude with the optimized electrodes.
- A 70 % reduction of total Pt loading was achieved by electro spray with better performance.
- The electrodes with lower Pt content demonstrated to be robust.

GRAPHICAL ABSTRACT



ARTICLE INFO

Keywords:

Sulfur depolarized electrolysis
Efficiency
Electro spray
Green hydrogen
Energy conversion

ABSTRACT

Sulfur dioxide depolarized electrolysis (SDE) is a promising technology for cost-effective green hydrogen production that can be used for the storage of intermittent renewable energies used to power the electrolyzer. The obtained hydrogen can be stored and used as a source for producing electricity in a fuel cell. However, high platinum loadings (around 2 mgPt cm⁻²) in the anode and cathode electrodes significantly contribute to the overall cost of the electrolyzer. This study aimed to optimize both electrodes using the electro spray technique for the deposition of ultra-low Pt loadings. The electrodes achieved a total platinum loading as low as 0.4 mgPt cm⁻² (0.3 mgPt cm⁻² for the anode and 0.1 mgPt cm⁻² for the cathode), an 80 % reduction compared to common platinum loadings. This reduction not only increased the hydrogen production rate (18 mL min⁻¹ with optimized electrodes vs. 4.7 mL min⁻¹ with non-optimized electrodes) but also decreased the production of hydrogen sulfide in the cathode, resulting in a hydrogen stream with higher purity. Overall, this study demonstrates the potential of electro spray for achieving low platinum loadings and improving the efficiency of SDE for green hydrogen production.

* Corresponding author.

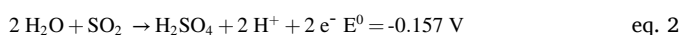
E-mail address: justo.lobato@uclm.es (J. Lobato).

1. Introduction

The rapid growth of the energy sector is the main cause of global warming due to the exponential increase in greenhouse gas emissions [1–3]. Consequently, governments are presenting policies to encourage the transition to a decarbonized energy sector. One clear example is the European Green Deal, with an ambitious objective of reaching zero net emissions of greenhouse gases for 2050 [4]. The development and integration of renewable energies (REs) are the obvious tools to meet this goal [5–7]. However, REs are facing some challenges that are slowing down their full integration into the grid [8]. They have an intermittent and unpredictable nature as they depend on weather conditions, and they are also variable in location [5,9]. In this scenario, energy storage technologies are key to complement REs to be successfully integrated into the grid, as they will help to provide a stable power output from REs. Among energy storage technologies, the use of hydrogen has emerged as one of the most promising alternatives [10]. The Hydrogen Roadmap [11], derived from the European Green Deal, states that “hydrogen is the best (or only) choice for at-scale decarbonization of selected segments in transport, industry and buildings”. The excess of electricity from REs needs to be transformed into a different energy, as electricity cannot be stored on a large scale. By using that excess of electricity to power a water electrolysis device, electricity can be converted into hydrogen as chemical energy [12–14]. Later, that hydrogen can be used in a fuel cell to produce electricity when required by demand. Proton exchange membrane (PEM) electrolysis is one of the alternatives for green hydrogen production, which, unlike liquid alkaline electrolysis, is efficient when operating with a variable power input. Nevertheless, the high cost of water electrolysis due to the high theoretical potential of 1.23 V vs. reference hydrogen electrode (RHE) and the use of precious metals such as platinum and iridium are impeding the large-scale implementation of this technology. The development of new methods for the splitting of water is one way to make the production of hydrogen by electrolysis more economically attractive. The Hybrid Sulfur (HyS) cycle uses SO₂ as an intermediary in the water-splitting reaction to lower the theoretical potential to a value as low as 0.157 V vs. RHE [15–17], which results in a lower energy input in the electrolysis step for the generation of the same amount of hydrogen. Moreover, the low required voltages allow for the use of carbon-based materials in the anode instead of titanium-based materials for (PEM) based water electrolysis. The HyS consists of three steps. The first step is the thermal decomposition of sulfuric acid (eq. (1)) at temperatures of around 900 °C which can be carried out using solar concentration energy or with spent heat generated in nuclear reactors. This is followed by a gas separation step to obtain a high-purity SO₂ stream.



The final step is the so-called sulfur depolarized electrolysis (SDE) (eq. (2) and eq. (3)) in which SO₂ and water react in the anode producing sulfuric acid and protons that cross the membrane to be reduced into hydrogen in the cathode. In this step, the excess of renewable energies can be used to produce hydrogen as an energy vector to store these energies when energy demand is low.



Although several catalysts have been studied for the SDE [18], platinum is the most efficient catalyst for the SDE electrolysis, and not iridium which is the main anode catalyst for PEM water electrolysis. The use of these precious metals accounts for a large part of the cost of the electrolyzer. One way of reducing the cost of the electrochemical cell is by changing the catalyst, however, only gold and palladium have shown acceptable performance for the SDE apart from Pt [19–21] which also have a high cost. Although gold shows better activity, its durability is

worse than that of palladium or platinum, and some works show different activity for Pd. Therefore, other approaches must be followed to reduce the cost of the catalyst layer. Recovering the spent platinum of the SDE will allow for a reduction of the investment in this metal for the electrolysis step, and some works are already exploring this idea [22, 23]. On the other hand, optimizing the deposition technique and lowering the catalyst loading will potentially decrease the total cost of the electrolyzer [24]. One of the ways to reach low platinum loadings with high performance is the deposition of the catalyst via the electro-spray deposition technique. In a previous work, our group demonstrated the feasibility of using electro-spray for the deposition of a platinum catalyst for the SDE in a half cell. Electro-spray was demonstrated to provide a larger electrochemical active area (ECSA) of the catalyst layer and also higher activity towards the SDE with ultra-low Pt loadings [25]. This technique has several advantages over other deposition methods such as producing a uniform layer with high precision and control over the deposition rate, contributing to a more efficient reaction with low catalyst loadings. Moreover, its versatility and scalability make electro-spray a powerful technique for catalyst deposition. A detailed review of this topic can be found elsewhere [26]. On the other hand, current approaches on the SDE processes aim to carry out this electrochemical reaction at temperatures higher than 100 °C using steam and gaseous SO₂, as preliminary modeling studies have demonstrated enhanced kinetics at those temperatures that result in higher hydrogen production rates. Currently, there are only a few studies that have investigated the SDE at temperatures higher than 100 °C [27,28], using a total catalyst loading between 1 mgPt cm⁻² and 2 mgPt cm⁻², and there is still a large knowledge gap of what occurs in a sulfur environment at those temperatures. In this context, this work intends to evaluate the electro-spray deposition technique and optimize the platinum loading of a high-temperature SDE single-cell electrolyzer. To do so, anodes and cathodes prepared using airbrush and electro-spray deposition will be tested and the electrochemical performance of the electrolyzer will be assessed. Moreover, as a novel aspect of this work, the hydrogen production rate and its purity will be shown and hence the efficiency of the process will be evaluated.

2. Materials and methods

2.1. Electrode preparation

Both anode and cathode were prepared by deposition of a catalytic ink composed of Pt/C (40 wt% Pt, Fuel Cell Store, USA), with polybenzimidazole (PBI) as ionomer (1.98 wt%, diluted from a 26 wt% solution using N,N-dimethylacetamide (DMAc), PBI Performance Products, USA), with a proportion of 1/20 related to the carbon support content, and DMAc as solvent (Merk, Germany). Various catalyst loadings were studied for the anode and cathode. For the anode catalyst loadings in the range of 0.5 mgPt cm⁻² and 0.1 mgPt cm⁻² were tested. And, for the cathode, the catalyst loading ranged between 0.3 mgPt cm⁻² and 0.05 mgPt cm⁻². The electrodes deposited by airbrush were prepared using an air gun loaded with the catalytic ink and connected to a N₂ (Air Liquide, Spain) used as carrier gas to deposit the ink onto a 25 cm² electrode (H23C2 GDL{Thickness 255 mm; Air Permeability 10 s; Resistivity 10 mΩ/cm²} Freudenberg, Germany) placed on a hot plate set up at 130 °C to evaporate the solvent. In the case of the electro-spray deposition, a Fluidnatek LE-50 {V_{Max} syringe 140 mL; Electrical Voltage drop up to 40 kV (up to +30 kV and –10 kV for the emitter and the collector, respectively); Flow rate between 0.1 and 1000 mL/h} (Bio-incia, Spain) was used. The electro-spray settings were the same as in our previous work [24]. Briefly, the ink flow rate was 800 μL h⁻¹ giving a weight gain of 1.8 mg/cycle, the injector voltage was 6 kV the collector voltage was set to 0 kV, and the distance between the needle (30 G) and the electrode was 2 cm. For both deposition techniques, the catalyst loading was adjusted by weighting the electrode before and after the deposition process.

2.2. SDE electrolyzer

For the experiments, a 25 cm² electrolyzer was assembled tightening the cell with a torque of 1 N m⁻² as described in previous works [28–30]. Briefly, it consists of two stainless steel endplates, two gold current collectors and two graphite bipolar plates with serpentine channels for both anode and cathode. For the electrodes, H23C2 GDL was used as gas diffusion and supporting layer (Freudenberg, Germany). The electrodes were sandwiched between a m-PBI membrane (50 μm dry thickness, PBI Performance Products, USA) with no previous hot pressing. The PBI membrane was doped overnight at 80 °C in 85 wt% H₃PO₄ (Merck, Germany), reaching an acid doping level of 11.4 mol of acid per repeating unit of PBI [29]. Before the assembly, the membrane was wiped using tissue paper to remove the excess of H₃PO₄. Moreover, 0.5 g of a 10 wt% H₃PO₄ solution was drop cast onto the electrodes and let dry overnight the day before the assembly to dope the PBI used as an ionomer in the inks.

2.3. SDE set-up and procedure

Before introducing SO₂ to the electrolyzer, the electrolyzer was heated to 110 °C, steam (0.2 mL min⁻¹ of liquid Mili-Q water) was fed to the anode and a mixture of N₂ (100 mL min⁻¹) and steam (0.5 mL min⁻¹ of liquid water) was fed to the cathode while applying a cell voltage of 0.6 V to prevent the crossover of SO₂. By doing this, time gaps of SO₂ entering the electrolyzer with no voltage are avoided. After a baseline with steam was obtained (around 5 min with a current value close to 0 A), a flow of 70 mL min⁻¹ of SO₂ (Nippon Gases, Spain) was mixed with the steam before entering the electrolyzer cell. For the break-in before the characterization, a constant voltage of 0.6 V was applied for 90 min. Electrochemical characterization was carried out at 110 °C, 120 °C, and 130 °C using a galvanostat/potentiostat PGSTAT204 equipped with a 20 A Booster and an impedance FRA32 module (AutoLab, Netherlands). Linear sweep voltammeteries were performed in the cell potential range of 0.4–1 V using a scan rate of 10 mV s⁻¹. Hydrogen production was measured at 0.6 V. Hydrogen rate and purity were measured by gas chromatography with a GC-2030 (Shimadzu, Japan) equipped with a Rxi-1ms column (L = 30 m; ID = 0.32 mm; DF = 0.50 μm) for sulfurous compounds (H₂S and SO₂) and a Rt-Msieve 5A column (L = 30 m; ID = 0.32 mm; DF = 30 μm) for small gas molecules (H₂, N₂, and O₂). Hydrogen faradaic efficiency was calculated using the real amount of produced hydrogen and the theoretical hydrogen production rate at 0.6 V at the measured current density *and applying the well-known Faraday law*. Before the measurements, the gas chromatograph was calibrated with different mixtures of N₂ and H₂. Electrochemical impedance spectroscopy (EIS) was performed at 0.6 V in the frequency range of 0.1–10,000 Hz with an amplitude equal to 10 % of the applied voltage (60 mV). EIS results were fitted using the NOVA 2.0 software to an R(RC) model (Fig. S1).

2.4. Optimization procedure

The anode and cathode were optimized based on polarization curve performance and also in terms of hydrogen production rate and purity using the following procedure. First, a baseline experiment was carried out fixing both anode and cathode platinum loadings at 0.7 mgPt cm⁻², using the conventional catalyst deposition technique of air-brush. This loading was selected based on our previous works that showed to be sufficient for the SDE [17, 18, 28–30]. Then, the anode was optimized by testing catalyst loadings of 0.5, 0.3, and 0.1 mgPt cm⁻² (with both airbrush and electro spray), while maintaining a cathode catalyst loading of 0.7 mgPt cm⁻² (deposited by airbrush). Once the anode was optimized, the investigated cathode catalyst loadings were 0.3, 0.1, and 0.05 mgPt cm⁻², prepared with airbrush and electro spray. When the cathode was optimized, the anode loading was also maintained in a catalyst loading of 0.7 mgPt cm⁻² (airbrush) to optimize the cathode in the same

conditions. The sample nomenclature follows the X-AG/ES-A/C, where X is the Pt loading, AG/ES refers to the deposition method being AG air-gun and ES electro spray, and A/C refers to which electrode is being optimized where A is anode and C is cathode. Table 1 shows the different combination of electrodes with which the electrolyzer was assembled to optimize the anode and cathode.

Finally, when the optimum catalyst loadings and deposition technique for the anode and cathode were selected, an experiment with both optimized electrodes (OE test) was carried out and the results were compared with the base scenario using a catalyst loading of 0.7 mgPt cm⁻² for both anode and cathode, deposited by air-brush. Moreover, a preliminary short-term stability test was performed once the evaluation of the performance of the SDE with the optimized electrodes at different temperatures was finished, the electrolyzer was kept at 120 °C and 0.6 V till 8.5 h of total operation.

3. Results

3.1. Anode optimization

The anode where the water splitting reaction occurs was the first catalyst layer to be optimized, since for the SDE process the anode is the limiting reaction (OER) [31–33]. Therefore, the catalyst loadings studied for this catalyst layer was 0.5–0.1 mgPt cm⁻² while for the cathode, where only the hydrogen evolution reaction (HER) occurs, the studied catalyst loading range was 0.3–0.05 mgPt cm⁻². A baseline experiment using 0.7 mgPt cm⁻² in both anode and cathode prepared by airbrush is shown in Fig. S2 catalyst. This loading was selected as that was the value employed for our previous SDE works [17, 28] and because is similar to other works published on this topic [34, 35]. For the baseline test (Fig. S2), lower performance was observed in the linear sweep voltammetry and in the production of hydrogen compared to 0.5AG_A (Table 1), attributed to agglomeration due to the higher catalyst loading (Fig. S4). For high loadings and elevated catalyst deposition times, particles tend to agglomerate as the electrical conductivity of the catalyst particles is higher than that of the carbon electrode. This aggregation effect was evidenced in our previous work where we tested electro sprayed electrodes in a half-cell [25], in that work it can be observed that a platinum loading higher than 0.3 mgPt cm⁻² causes particle agglomeration on the carbon paper electrode (Fig. S4). Regarding the linear sweep voltammetry for the anode optimization, Fig. 1 shows the results obtained at 110 °C, 120 °C and 130 °C. For the airbrush deposition, 0.5AG_A and 0.3AG_A show similar results with slightly better performance for 0.5AG_A as it reaches a current density of 0.34 A cm⁻² at 1 V compared to 0.32 A cm⁻² for 0.3AG_A at 110 °C. The study demonstrates that a platinum loading of 0.3 mgPt cm⁻² is adequate for conducting the SDE as no kinetic loss or mass transport limitations are observed. However, when the

Table 1

Catalyst loadings and deposition techniques were employed for the optimization of the electrolyzer electrodes.

Test	Anode deposition technique	Cathode deposition technique	Anode platinum loading [mgPt cm ⁻²]	Cathode platinum loading [mgPt cm ⁻²]
0.5AG _A	Airbrush	Airbrush	0.5	0.7
0.3AG _A	Airbrush	Airbrush	0.3	0.7
0.1AG _A	Airbrush	Airbrush	0.1	0.7
0.5ES _A	Electrospray	Airbrush	0.5	0.7
0.3ES _A	Electrospray	Airbrush	0.3	0.7
0.1ES _A	Electrospray	Airbrush	0.1	0.7
0.3AG _C	Airbrush	Airbrush	0.7	0.3
0.1AG _C	Airbrush	Airbrush	0.7	0.1
0.05AG _C	Airbrush	Airbrush	0.7	0.05
0.3ES _C	Airbrush	Electrospray	0.7	0.3
0.1ES _C	Airbrush	Electrospray	0.7	0.1
0.05ES _C	Airbrush	Electrospray	0.7	0.05

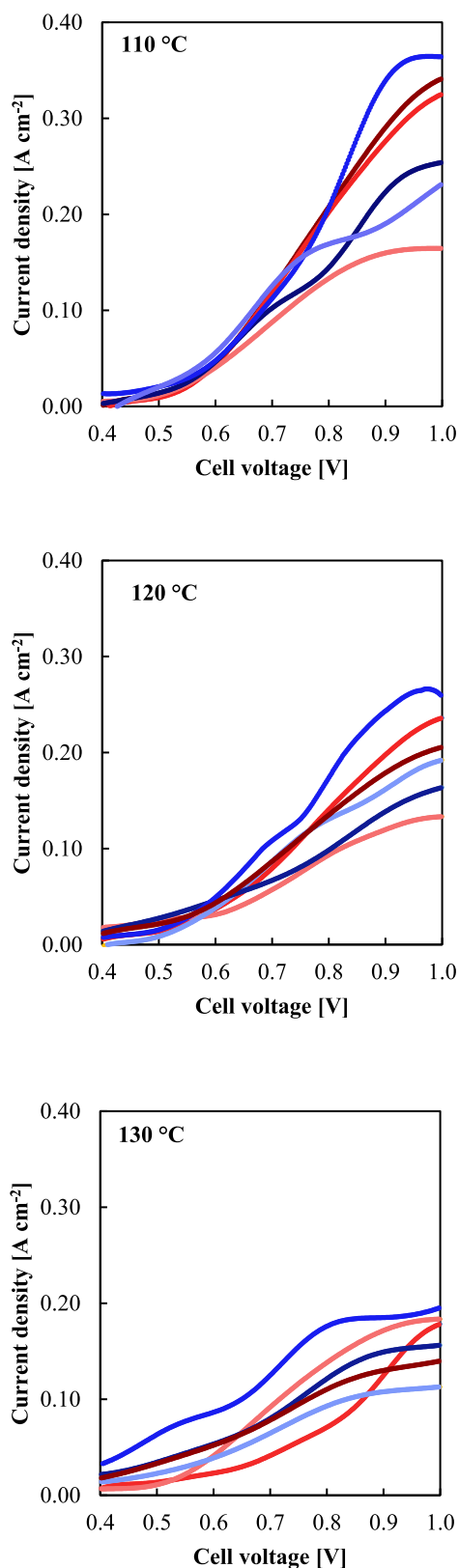
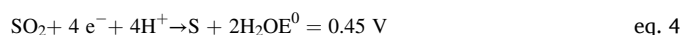


Fig. 1. Linear sweep voltammeteries for the electrodes employed in the anode optimization at different temperatures. Dark red: 0.5AG_A; Red: 0.3AG_A; Light red: 0.1AG_A. Dark blue: 0.5ES_A; Blue: 0.3ES_A; Light blue: 0.1ES_A. (For interpretation of the references to colour in this figure legend, the reader is referred to the Web version of this article.)

anode loading is reduced to 0.1 mgPt cm⁻² (0.1AG_A), there is a noticeable decline in performance, particularly evident for cell voltages exceeding 0.7 V. This suggests that a platinum loading of 0.1 mgPt cm⁻² for the anode is insufficient, as indicated by a plateau in performance attributed to mass transport issues. Electrodes prepared using electro-spray exhibit a different trend. The polarization curve for 0.5ES_A displays poorer performance compared to 0.5AG_A and 0.3AG_A, with a maximum current density of 0.25 A cm⁻² at 1 V. As evidenced in our previous work [25], higher catalyst loadings than 0.3 mgPt cm⁻², when prepared by electro-spray, lead to catalyst particle agglomeration. Conversely, 0.3ES_A at 110 °C demonstrates a maximum current density exceeding 0.36 A cm⁻², almost 10 % higher than its 0.5AG_A counterpart, despite using 40 % less platinum. This improvement is attributed to the enhanced catalyst dispersion achieved through electro-spray. Similarly, while 0.1ES_A exhibits significantly lower performance compared to 0.3ES_A due to inadequate platinum amount, its improved dispersion relative to 0.1AG_A results in better performance.



At 120 °C, side reactions (Eqs. (4)–(6)) in the anode sulfur environment [19,20,36] cause a decline in overall performance. While eq. (4) is an electrochemical reaction, eqs. (5) and (6) are chemical reactions. Nonetheless, 0.3ES_A maintains the highest performance with a current density of 0.26 A cm⁻² at 1 V, surpassing both 0.3AG_A and 0.5AG_A by 10 % and 30 % respectively. Finally, at 130 °C, polarization curves show erratic results. For instance, 0.1AG_A, previously exhibiting the worst performance, now ranks as the second-best scenario. This unexpected behavior may be attributed to the poor catalytic activity of 0.1AG_A, unaffected by side reactions that are more pronounced at 130 °C. Consequently, results at 130 °C were excluded from selecting the optimal loading and deposition technique for the anode. Regarding EIS results (Table S1), they corroborate the findings from linear sweep voltammetry. Ohmic resistance (R_{Ω}) decreases slightly with temperature, reflecting the decrease in material resistance and the increased conductivity of phosphoric acid-doped PBI membranes [37,38]. However, charge transfer resistance (R_p) increases with temperature, suggesting that SDE kinetics do not improve with temperature or that enhanced side reactions hinder SDE behavior. Electro-spray-prepared electrodes tend to have slightly lower R_p values, indicating better dispersion. Moreover, a low catalyst loading of 0.1 mgPt cm⁻² causes a significant increase in charge transfer resistance at 120 °C, not observed in the case of higher catalyst loadings.

Fig. 2 shows the hydrogen production rate and the faradaic efficiency for the set of experiments performed for the anode optimization.

As expected, at 110 °C, for the highest studied catalyst production rate and efficiency are obtained for 0.5AG_A. Moreover, the faradaic efficiency towards hydrogen production is only 65 % for 0.5ES_A. This is explained as a lower performance means that less SO₂ reacts in the anode and can cross to the cathode consuming protons and electrons to form sulfur and sulfidric acid. Similarly, for the lowest catalyst loading of 0.1 mgPt cm⁻², the faradaic efficiency drops to values as low as 65 % for 0.1AG_A. In this case, this reduced efficiency is due to the low amount of catalyst. For 0.3 mgPt cm⁻², the improved catalyst dispersion enhances hydrogen production, with a 64 % higher hydrogen rate than for 0.3AG_A and 13 % higher than 0.5AG_A with 40 % less catalyst. At 120 °C the trend is similar, however, due to the increase in temperature, other side reactions are also enhanced which decrease hydrogen production as also was observed for linear sweep voltammeteries. Higher temperatures shorten the difference between a catalyst loading of 0.1 mgPt cm⁻² and 0.3 mgPt cm⁻², and, while the hydrogen rate for 0.3AG_A is the same at both temperatures, for 0.3ES_A there is a substantial decrease. The reason is that for 0.3AG_A the catalyst dispersion is limiting the reaction rate,

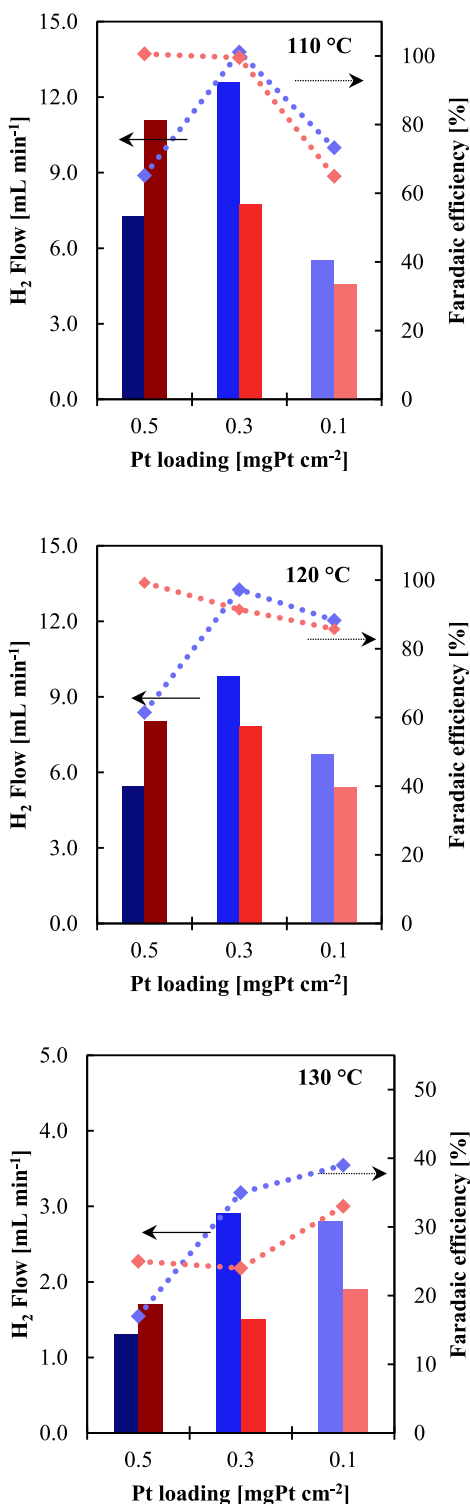


Fig. 2. Hydrogen production rates and faradaic efficiency for the tests performed for the anode optimization at different temperatures. Dark red: 0.5AG_A; Red: 0.3AG_A; Light red: 0.1AG_A. Dark blue: 0.5ES_A; Blue: 0.3ES_A; Light blue: 0.1ES_A. Red dotted line: faradaic efficiency for the airbrush deposition technique. Blue dotted line: faradaic efficiency for the electro spray deposition technique. (For interpretation of the references to colour in this figure legend, the reader is referred to the Web version of this article.)

therefore, the increase in temperature has little effect in this case. On the other hand, for 0.3ES_A the kinetics and side reactions are the limiting factors affecting the performance of the electrolyzer. Finally, at 130 °C, the concentration of H₂S exponentially increases in the cathode (Table S4) which hinders the production of hydrogen. For that reason, faradaic efficiencies are below 40 % while at 110 °C and 120 °C, they were close to 100 %. However, 0.1ES_A and 0.3ES_A show promising performance with the highest hydrogen production rates at this temperature. Therefore, as a partial conclusion, 0.3ES_A is considered as the optimized anode catalyst loading deposition due to the polarization curves results and the hydrogen production rates.

3.2. Cathode optimization

Once the anode electrode was optimized, the same protocol was followed to optimize the cathode. To perform the optimization in the same conditions as for the anode, the catalyst loading was fixed to 0.7 mgPt cm⁻² deposited with airbrush in the anode. For the cathode, as the HER is the only reaction that will occur according to eq (3), lower catalyst loadings are needed. Consequently, the studied catalysts loadings were 0.3 mgPt cm⁻², 0.1 mgPt cm⁻² and 0.05 mgPt cm⁻². Fig. 3 shows the polarization curves for the different cathode catalyst layers. In general, as occurred for the anode optimization, increasing temperature did not translate to higher maximum current densities due to the enhancement of secondary reactions at higher temperatures. At 110 °C the best performance is obtained for 0.1ES_C (0.38 A cm⁻²) followed by 0.05ES_C (0.34 A cm⁻²) and 0.1AG_C (0.33 A cm⁻²). At this temperature, the two lowest loadings deposited by electro spray show the best performance due to the excellent dispersion of the catalyst and highest values of ECSA as it can be seen in Table S2, but at a loading of 0.05 mgPt cm⁻² is negatively affecting the performance of the electrolyzer. Consequently, the worse dispersion of 0.05AG_C over 0.05ES_C explains the poorer performance of the former. Regarding the highest catalyst loadings, the inability of electro spray to homogeneously disperse that amount of catalyst (0.3ES_C) results in a maximum current density of 0.27 A cm⁻², which is 40 % lower than for 0.1ES_C with three times less platinum. Moreover, when compared with the conventional 0.3AG_C the difference is an astonishing 81 %. Interesting results are obtained at 120 °C for the 0.1 mgPt cm⁻² loading prepared with both techniques as the maximum current densities of those two cases are higher than any of the experiments carried out for the anode optimization. In other words, the increase of temperature did not affect as significantly as for the previous set of experiments. This is attributed to the inhibition of side reactions in the cathode that poison the catalyst due to a much lower amount of platinum. This is further confirmed by the results at 130 °C where the trend is clear. For 0.3AG_C and 0.3ES_C, the high amount of platinum also promotes the production of H₂S as confirmed by the chromatography measurements (Table S3). The best results and following the trend of the results at 110 °C and 120 °C, were obtained for 0.1AG_C and 0.1ES_C, with a superior performance of the electrode prepared by electro spray. Moreover, the production of H₂S drastically decreases confirming that side reactions generating this poisoning species are limited. This could be explained taking into account that the reduction of sulfur dioxide to sulfur is more difficult than the reduction of protons to hydrogen (0.45 V vs 0.0 V, as it can be seen in eq (4)) and hence, when there are less particles of catalyst available in the cathode electrode the production of sulfur based compounds is minimized. For 0.05AG_C and 0.05ES_C the results are identical, however, such a low platinum loading affects the kinetics of the cathode resulting in worse performance than for the 0.1 mgPt cm⁻² loading. On the other hand, EIS results for the cathode optimization (Table S1) demonstrate the beneficial effect of decreasing the catalyst loading, as for 0.1 mgPt cm⁻² and 0.05 mgPt cm⁻² the charge transfer resistance decreases from 110 °C to 120 °C, which did not happen in the anode optimization experiments.

Fig. 4 shows the hydrogen production rates and faradaic efficiency for the cathode optimization experiments. In this case, the electro spray

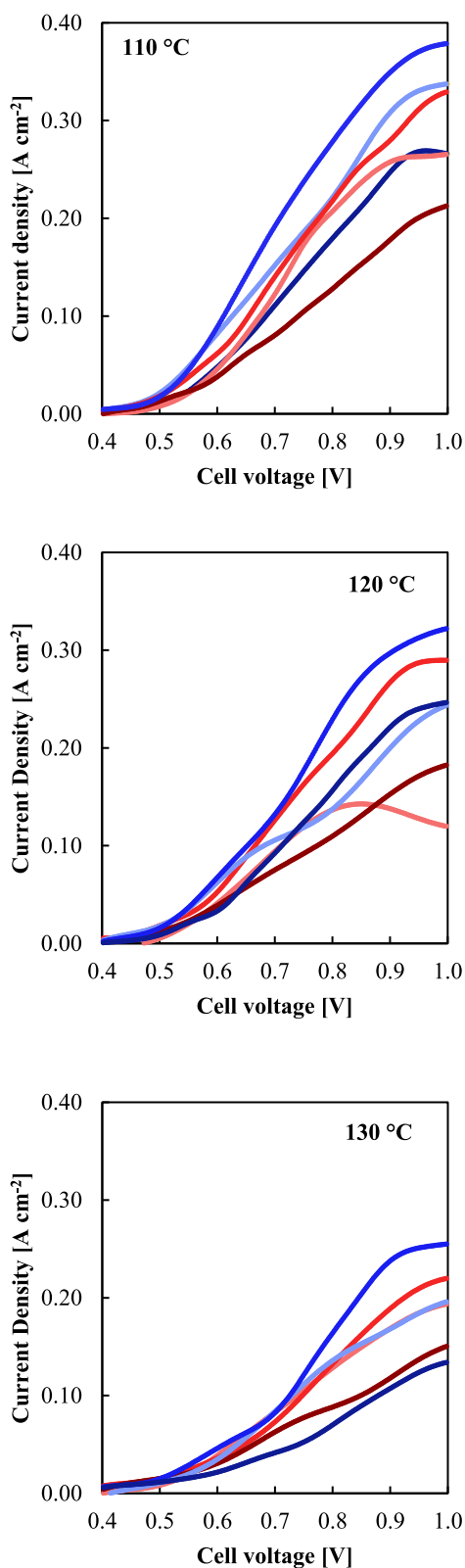


Fig. 3. Linear sweep voltammeteries for the electrodes employed in the cathode optimization at different temperatures. Dark red: 0.3AG_C; Red: 0.1AG_C; Light red: 0.05AG_C. Dark blue: 0.3ES_C; Blue: 0.1ES_C; Light blue: 0.05ES_C. (For interpretation of the references to colour in this figure legend, the reader is referred to the Web version of this article.)

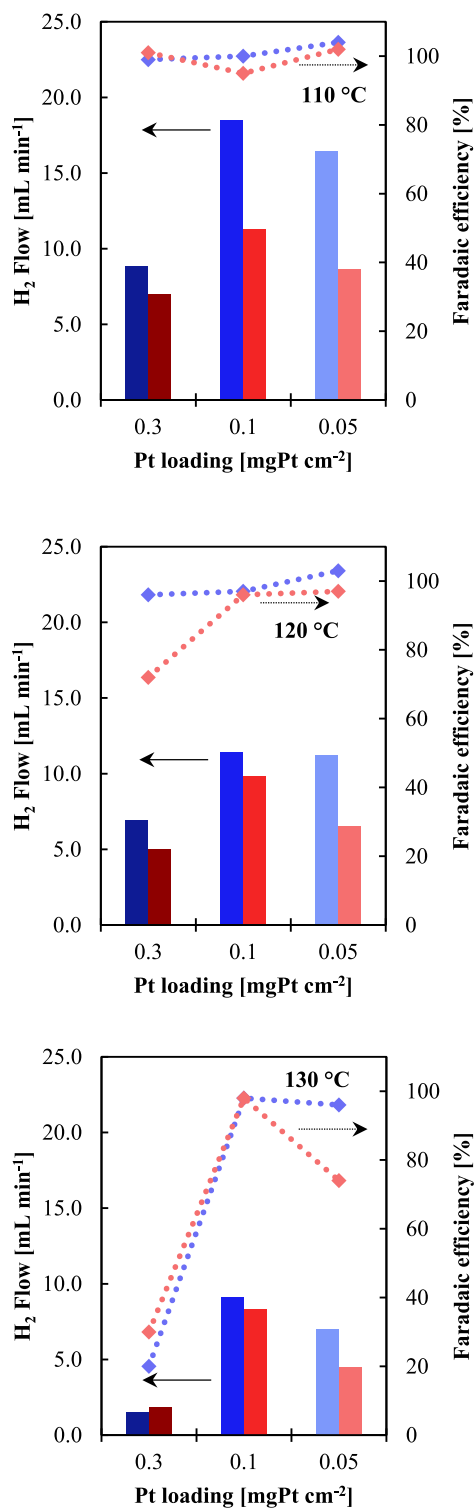


Fig. 4. Hydrogen production rates and faradaic efficiency for the tests performed for the cathode optimization at different temperatures. Dark red: 0.5AG_A; Red: 0.3AG_A; Light red: 0.1AG_A. Dark blue: 0.5ES_A; Blue: 0.3ES_A; Light blue: 0.1ES_A. Red dotted line: faradaic efficiency for the airbrush deposition technique. Blue dotted line: faradaic efficiency for the electro spray deposition technique. (For interpretation of the references to colour in this figure legend, the reader is referred to the Web version of this article.)

technique shows superior performance in every pair of electrodes in terms of hydrogen production. At 110 °C, all the samples show an expected faradaic efficiency of around 100 %. However, the performance of 0.1ES_C is far superior to the best cathode prepared by airbrush which is 0.1AG_C, producing 64 % more hydrogen. At 120 °C, electrospray is still the best deposition technique for the cathode, as in this case the catalyst loadings were lower than the studied for the anode. With a similar hydrogen production rate for 0.1ES_C and 0.05ES_C. Nevertheless, the most interesting result is obtained at 130 °C. While the faradaic efficiency for 0.3ES_C and 0.3AG_C follows the trend observed for the anode optimization with values close to 30 % and very low hydrogen production rates, this efficiency rises to values close to 100 % for the lowest platinum loadings. This data, combined with the H₂S measurements confirm that the production of H₂S is avoided with the use of low platinum loadings in the cathode. Moreover, it can be stated that the deposition technique did not affect this behaviour as it occurs for both electrospray and airbrush. Regarding performance, as for the previous temperatures, the best results were obtained for 0.1ES_C. In terms of the selection of the optimum catalyst loading and deposition technique for the cathode, 0.1ES_C and 0.05ES_C did not show very different hydrogen production rates even though the difference in platinum loading is double. However, considering the polarization curves results and the slightly higher hydrogen production rate for 0.1ES_C, this loading and technique were selected as optimum for the experiment in which the electrolyzer was assembled with both the optimized anode and cathode electrodes.

3.3. Short-term electrolysis with the optimized electrodes

Once both electrodes were optimized, the SDE electrolyzer was assembled with an anode with a platinum loading of 0.3 mgPt cm⁻² and a cathode with a loading of 0.1 mgPt cm⁻² both of them prepared with the electrospray technique (OE test). As a comparison, an experiment was carried out with electrodes with a catalyst loading of 0.7 mgPt cm⁻² using airbrush deposition, which was the base scenario (BS test). This means that the total platinum loading for the OE test was 0.4 mg Pt cm⁻², which is 3.5 times less platinum than the 1.4 mgPt cm⁻² used in the BS test. Firstly, the electrolyzer was characterized at 110 °C, 120 °C and 130 °C. As expected, the performance in the OE test is superior to the BS test even though the amount of catalyst is considerably lower. For instance, polarization curves (Fig. 5) show that the maximum current density is always higher for the OE test at 1V (0.42, 0.34, and 0.28 A cm⁻² vs 0.29, 0.29, and 0.12 A cm⁻²). What is more, for the BS test the polarization curve at 130 °C shows poor performance caused by the side reactions in the cathode, while for the experiment with both electrodes prepared by electrospray, the performance is also affected by side reactions but with considerably better current density values than for the BS test. It is interesting to observe the trend in the polarization curves for the OE test, as they suffer a systematic decrease when increasing temperature. Proving that the best results are obtained at the lowest tested temperature of 110 °C.

Table 2 shows the actual production of hydrogen for both experiments at 110 °C, 120 °C and 130 °C and during the short-term durability test in which the cell potential was held to 0.6 V. For both cases, the hydrogen production rate decreases with temperature because of the influence of side reactions that lead to the adsorption of sulfur species in the catalyst surface lowering the performance. However, for the case of the OE test, the decrease is only 30 % compared to an 85 % decrease for the base scenario. As previously commented, side reactions consuming protons, electrons, and hydrogen are enhanced at high temperatures and high cathode platinum loadings. In fact, at 130 °C, when the H₂S production is boosted, the H₂S rate of the BS test experiment is 6.7 higher than for the OE test (Table S5 shows the production of H₂S in ppm). This again proves that a lower catalyst loading worsens the kinetics of the cathode side reactions. Therefore, at 130 °C only 1.66 mL min⁻¹ of hydrogen is produced for the BS but 14.37 mL min⁻¹ for the OE (which is

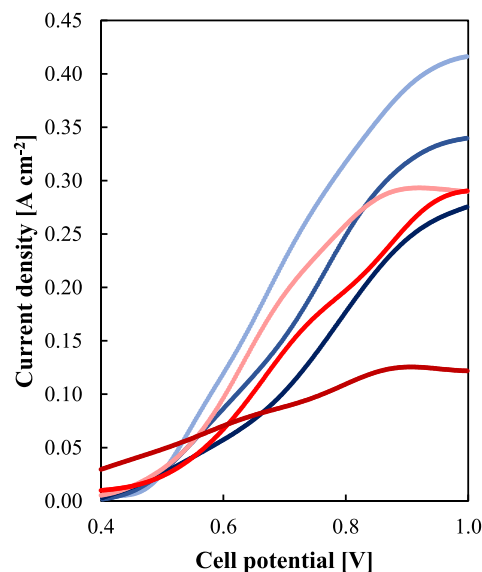


Fig. 5. Linear sweep voltammeteries for the electrodes employed in the OE test and BS test. Dark red: BS at 130 °C; Red: BS at 120 °C; Light red: BS at 110 °C. Dark blue: OE at 130 °C; Blue: OE at 120 °C; Light blue: OE at 110 °C.

Table 2

Hydrogen production rates for the OE test and BS test.

Temperature	OE test		BS test	
	H ₂ [mL min ⁻¹]	H ₂ S [mL min ⁻¹]	H ₂ [mL min ⁻¹]	H ₂ S [mL min ⁻¹]
110 °C	20.31	0.022	11.09	0.06
120 °C	18.63	0.037	8.04	0.29
130 °C	14.37	0.205	1.66	1.37
120 °C (t = 4h)	17.12	0.025	8.58	0.26
120 °C (t = 5.5h)	17.55	0.019	4.68	0.27
120 °C (t = 7h)	18.03	0.020	5.01	0.33
120 °C (t = 8.5h)	17.96	0.020	4.37	0.71

a hydrogen production 8.7 times higher). Regarding the short-term durability test, it is clear that the higher rate of side reactions for the BS test constantly poisons the cathode catalyst layer as demonstrated by the hydrogen production rate decrease over time, with a final hydrogen rate 50 % lower than the first measured value. On the other hand, for the OE test, the hydrogen production rate maintains a constant value over the length of the experiment. It is also interesting to see that the first measurement shows a hydrogen rate of 17.12 mL min⁻¹ which then increases to 17.96 mL min⁻¹ for the final measurement. Indicating that the poisoning that could have occurred at 130 °C is not irreversible as the measured hydrogen flow slightly increases over time. Furthermore, the production of H₂S as a side product is constant for the OE test, while for the BS test, the measured H₂S flow increases over time. Demonstrating that with an optimized catalyst deposition and a catalyst loading around 3.5 times lower than that employed in most of the SDE published works, not only the electrochemical performance is improved but also the hydrogen production rate. What is more, the production of poisoning side products is also limited. Moreover, Table S3 shows the beneficial impact of the optimized electrodes on the charge transfer resistance, with values half of that observed for the BS test. The enhanced catalyst deposition by electro-spray and the lower catalyst loading in the anode that prevents the formation of H₂S explain these results.

On the other hand, it is difficult to compare these results related to hydrogen production and faradaic efficiency with others published in

the literature using the same technology as they only show the current density but not the hydrogen production. However, in this work the need of measuring hydrogen purity is shown to be paramount to evaluate the overall performance of this technology and not just look at electrolyzer performance.

4. Conclusions

Electrospray is a promising and reliable catalyst deposition technique to dramatically lower the catalyst loading in the electrodes of the SDE electrolyzer that could also be extrapolated to other electrochemical processes to produce hydrogen as a renewable energy storage process. In this work, the catalyst loading was decreased from 0.7 mgPt cm⁻² to 0.3 mgPt cm⁻² in the anode and from 0.7 mgPt cm⁻² to 0.1 mgPt cm⁻² in the cathode without losing electrolyzer performance while increasing the hydrogen production rate. Moreover, it was demonstrated that the cathode side reactions caused by SO₂ crossover are partially prevented by using lower catalyst loadings while the hydrogen production rate is not affected, resulting in a lower amount of side products that can poison the catalyst.

CRedit authorship contribution statement

Sergio Diaz-Abad: Writing – original draft, Methodology, Investigation, Formal analysis. **Iñaki Requena:** Writing – original draft, Investigation. **Manuel A. Rodrigo:** Writing – review & editing, Supervision, Funding acquisition. **Justo Lobato:** Writing – review & editing, Supervision, Funding acquisition, Conceptualization.

Declaration of competing interest

On behalf of all coauthors, I declare that this paper has no conflict of interest. It was only submitted to the journal *Energy* and the financial supporting agencies have been included in the acknowledgements. The submitted file has been approved by all coauthors.

Data availability

Data will be made available on request.

Acknowledgments

This research was funded by the Junta de Comunidades de Castilla-La Mancha and the FEDER e EU Program, Project ASEPHAM. Grant number “SBPLY/17/180501/000330”. This work also belongs to project PID2019-107271RB-I00 granted by MCIN/AEI/10.13039/501100011033/and European Union “NextGenerationEU/PRTR”. Therefore, these Institutions are gratefully acknowledged. Sergio Diaz also acknowledges the grant 2018/12504 from the University of Castilla-La Mancha.

Appendix A. Supplementary data

Supplementary data to this article can be found online at <https://doi.org/10.1016/j.jpowsour.2024.234513>.

References

- N.L. Panwar, S.C. Kaushik, S. Kothari, Role of renewable energy sources in environmental protection: a review, *Renew. Sustain. Energy Rev.* 15 (2011) 1513–1524, <https://doi.org/10.1016/j.rser.2010.11.037>.
- N.S. Lewis, D.G. Nocera, Powering the planet: chemical challenges in solar energy utilization, *Proc. Natl. Acad. Sci. USA* 103 (2006) 15729–15735, <https://doi.org/10.1073/pnas.0603395103>.
- J.M. Thomas, P.P. Edwards, P.J. Dobson, G.P. Owen, Decarbonising energy: the developing international activity in hydrogen technologies and fuel cells, *J. Energy Chem.* 51 (2020) 405–415, <https://doi.org/10.1016/j.jechem.2020.03.087>.
- European Commission, The European Green Deal, vol. 53, European Commission, 2019, p. 24, <https://doi.org/10.1017/CBO9781107415324.004>.
- S. Sridhar, S.R. Salkuti, Development and future scope of renewable energy and energy storage systems, *Smart Cities* 5 (2022) 668–699, <https://doi.org/10.3390/smartcities5020035>.
- M. Ji, J. Wang, Review and comparison of various hydrogen production methods based on costs and life cycle impact assessment indicators, *Int. J. Hydrogen Energy* 46 (2021) 38612–38635, <https://doi.org/10.1016/j.ijhydene.2021.09.142>.
- B. Dunn, H. Kamath, J.M. Tarascon, Electrical energy storage for the grid: a battery of choices, *Science* 334 (1979 2011) 928–935, <https://doi.org/10.1126/science.1212741>.
- A. Bilodeau, K. Agbossou, Control analysis of renewable energy system with hydrogen storage for residential applications, *J. Power Sources* 162 (2006) 757–764, <https://doi.org/10.1016/j.jpowsour.2005.04.038>.
- Amrouche S. Ould, D. Rekioua, T. Rekioua, S. Bacha, Overview of energy storage in renewable energy systems, *Int. J. Hydrogen Energy* 41 (2016) 20914–20927, <https://doi.org/10.1016/j.ijhydene.2016.06.243>.
- R. Mulla, C.W. Dunnill, Powering the hydrogen economy from waste heat: a review of heat-to-hydrogen concepts, *ChemSusChem* 12 (2019) 3882–3895, <https://doi.org/10.1002/cssc.201901426>.
- Fuel Cells and Hydrogen Joint Undertaking (FCH), Hydrogen Roadmap Europe, <https://doi.org/10.2843/249013>, 2019.
- S.E. Hosseini, M.A. Wahid, Hydrogen production from renewable and sustainable energy resources: promising green energy carrier for clean development, *Renew. Sustain. Energy Rev.* 57 (2016) 850–866, <https://doi.org/10.1016/j.rser.2015.12.112>.
- M. Carmo, D.L. Fritz, J. Mergel, D. Stolten, A comprehensive review on PEM water electrolysis, *Int. J. Hydrogen Energy* 38 (2013) 4901–4934, <https://doi.org/10.1016/j.ijhydene.2013.01.151>.
- C.J. Winter, J. Nitsch, *Hydrogen as an Energy Carrier: Technologies, Systems, Economy*, Springer, Berlin Heidelberg, 2012.
- S. Charton, J. Janvier, P. Rivalier, E. Chaînet, J.P. Caire, Hybrid sulfur cycle for H₂ production: a sensitivity study of the electrolysis step in a filter-press cell, *Int. J. Hydrogen Energy* 35 (2010) 1537–1547, <https://doi.org/10.1016/j.ijhydene.2009.12.046>.
- M.B. Gorensak, C. Corgnale, W.A. Summers, Development of the hybrid sulfur cycle for use with concentrated solar heat. I. Conceptual design, *Int. J. Hydrogen Energy* 42 (2017) 20939–20954, <https://doi.org/10.1016/j.ijhydene.2017.06.241>.
- S. Díaz-Abad, M.A. Rodrigo, J. Lobato, First approaches for hydrogen production by the depolarized electrolysis of SO₂ using phosphoric acid doped polybenzimidazole membranes, *Int. J. Hydrogen Energy* 46 (2021) 29763–29773, <https://doi.org/10.1016/j.ijhydene.2021.06.117>.
- S. Díaz-Abad, M. Millán, M.A. Rodrigo, J. Lobato, Review of anodic catalysts for SO₂ depolarized electrolysis for “green hydrogen” production, *Catalysts* 9 (2019) 63, <https://doi.org/10.3390/catal9010063>.
- J.A. O'Brien, J.T. Hinkley, S.W. Donne, Electrochemical oxidation of aqueous sulfur dioxide II. Comparative studies on platinum and gold electrodes, *J. Electrochem. Soc.* 159 (2012) 585–593, <https://doi.org/10.1149/2.060209jes>.
- J.A. Allen, G. Rowe, J.T. Hinkley, S.W. Donne, Electrochemical aspects of the Hybrid Sulfur Cycle for large scale hydrogen production, *Int. J. Hydrogen Energy* 39 (2014) 11376–11389, <https://doi.org/10.1016/j.ijhydene.2014.05.112>.
- K. Scott, W.M. Taama, Investigation of anode materials in the anodic oxidation of sulphur dioxide in sulphuric acid solutions, *Electrochim. Acta* 44 (1999) 3421–3427, [https://doi.org/10.1016/S0013-4686\(99\)00057-2](https://doi.org/10.1016/S0013-4686(99)00057-2).
- M.A. Montiel, R. Granados, S. Díaz-Abad, C. Sáez, C.M. Fernández-Marchante, M. A. Rodrigo, et al., Towards a circular economy for Pt catalysts. Case study: Pt recovery from electrodes for hydrogen production, *Appl. Catal., B* 327 (2023) 122414, <https://doi.org/10.1016/j.apcatb.2023.122414>.
- R. Granados-Fernández, M.A. Montiel, S. Díaz-Abad, M.A. Rodrigo, J. Lobato, Platinum recovery techniques for a circular economy, *Catalysts* 11 (2021), <https://doi.org/10.3390/catal11080937>.
- S. Martin, Q. Li, J.O. Jensen, Lowering the platinum loading of high temperature polymer electrolyte membrane fuel cells with acid doped polybenzimidazole membranes, *J. Power Sources* 293 (2015) 51–56, <https://doi.org/10.1016/j.jpowsour.2015.05.031>.
- I. Fouzai, M. Radaoui, S. Díaz-Abad, M.A. Rodrigo, J. Lobato, Electrospray deposition of catalyst layers with ultralow Pt loading for cost-effective H₂ production by SO₂ electrolysis, *ACS Appl. Energy Mater.* (2022), <https://doi.org/10.1021/acsaem.1c03672>.
- S. Martin, B. Martinez-Vazquez, P.L. Garcia-Ybarra, J.L. Castillo, Peak utilization of catalyst with ultra-low Pt loaded PEM fuel cell electrodes prepared by the electrospray method, *J. Power Sources* 229 (2013) 179–184, <https://doi.org/10.1016/j.jpowsour.2012.12.029>.
- R. Peach, H.M. Krieg, A.J. Kröger, D. Bessarabov, J. Kerres, Novel cross-linked PBI-blended membranes evaluated for high temperature fuel cell application and SO₂electrolysis, *Mater. Today Proc.* 5 (2018) 10524–10532, <https://doi.org/10.1016/j.matpr.2017.12.384>.
- S. Díaz-Abad, M.A. Rodrigo, C. Sáez, J. Lobato, Enhancement of the green H₂ production by using TiO₂ composite polybenzimidazole membranes, *Nanomaterials* 12 (2022) 2920, <https://doi.org/10.3390/nano12172920>.
- S. Diaz-abad, S. Fernández-Mancebo, M.A. Rodrigo, J. Lobato, Characterization of PBI/graphene oxide composite membranes for the SO₂ depolarized electrolysis at high temperature, *Membranes* 12 (2022) 116, <https://doi.org/10.3390/membranes12020116>.
- S. Díaz-Abad, S. Fernández-Mancebo, M.A. Rodrigo, J. Lobato, Enhancement of SO₂ high temperature depolarized electrolysis by means of graphene oxide

- composite polybenzimidazole membranes, *J. Clean. Prod.* 363 (2022), <https://doi.org/10.1016/j.jclepro.2022.132372>.
- [31] M.N.I. Salehmin, T. Husaini, J. Goh, A.B. Sulong, High-pressure PEM water electrolyser: a review on challenges and mitigation strategies towards green and low-cost hydrogen production, *Energy Convers. Manag.* 268 (2022) 115985, <https://doi.org/10.1016/j.enconman.2022.115985>.
- [32] S. Shiva Kumar, V. Himabindu, Hydrogen production by PEM water electrolysis – a review, *Mater. Sci. Energy Technol.* 2 (2019) 442–454, <https://doi.org/10.1016/j.mset.2019.03.002>.
- [33] P. Nikolaidis, A. Poullickas, A comparative overview of hydrogen production processes, *Renew. Sustain. Energy Rev.* 67 (2017) 597–611, <https://doi.org/10.1016/j.rser.2016.09.044>.
- [34] M.B. Gorenssek, B. Meekins, H. Colón-Mercado, J. Weidner, Parametric study of operating conditions of an SO₂-depolarized electrolyzer, *Int. J. Hydrogen Energy* 45 (2020) 22408–22418, <https://doi.org/10.1016/j.ijhydene.2020.06.067>.
- [35] J.L. Steimke, T.J. Steeper, H.R. Colón-Mercado, M.B. Gorenssek, Development and testing of a PEM SO₂-depolarized electrolyzer and an operating method that prevents sulfur accumulation, *Int. J. Hydrogen Energy* 40 (2015) 13281–13294, <https://doi.org/10.1016/j.ijhydene.2015.08.041>.
- [36] J.A. O'Brien, J.T. Hinkley, S.W. Donne, S.E. Lindquist, The electrochemical oxidation of aqueous sulfur dioxide: a critical review of work with respect to the hybrid sulfur cycle, *Electrochim. Acta* 55 (2010) 573–591, <https://doi.org/10.1016/j.electacta.2009.09.067>.
- [37] X. Chen, G. Qian, M.A. Molle, B.C. Benicewicz, H.J. Ploehn, High temperature creep behavior of phosphoric acid-polybenzimidazole gel membranes, *J. Polym. Sci. B Polym. Phys.* 53 (2015) 1527–1538, <https://doi.org/10.1002/polb.23791>.
- [38] J.A. Mader, B.C. Benicewicz, S. Carolina, Sulfonated polybenzimidazoles for high temperature PEM, *Fuel Cell.* 49 (2010) 6706–6715, <https://doi.org/10.1021/ma1009098>.